J. Fluid Mech. (2025), *vol.* 1024, F1, doi:10.1017/jfm.2025.10791

JFM FOCUS ON FLUIDS

A step beyond the tryptic of acoustic streaming

Valéry Botton[1]

[1]INSA Lyon, CNRS, Ecole Centrale de Lyon, Université Claude Bernard Lyon 1, LMFA, UMR5509, Villeurbanne 69621, France

Corresponding author: Valery Botton, valery.botton@insa-lyon.fr

(Received 21 September 2025; revised 21 September 2025; accepted 1 October 2025)

The path followed since Faraday's first observations of acoustic streaming has led to a modern picture of this field as split into separate panels of a tryptic: standing acoustic waves in a channel with uniform background density, known as Rayleigh–Schlichting streaming, with stratified background density, known as baroclinic streaming, and acoustic waves progressing far from the walls under the shape of an attenuated beam, known as Eckart streaming. In their theoretical work, Mushthaq *et al.* (2025 *J. Fluid Mech.* **1017**, A32) describe in a single continuous parameter space both Rayleigh–Schlichting and baroclinic streaming, thus making a decisive step forward in the frontier between two of these panels. Dealing with a stratification of thermal origin, they identify the level of heating above which baroclinic streaming becomes of the same order of magnitude or greater than Rayleigh–Schlichting streaming. They also depict the major part played by the channel size to wavelength ratio in this problem. This work will be of great help in designing the next generation of experiments concerning acoustic streaming and acoustic management of heat transfer. It is of interest for engineering fields like microfluidics, electronics cooling and biomedical applications. It can also serve as an inspiring basis for academic works in which waves are crossed with stratification.

Key words: stratified flows, baroclinic flows

1. A path from Faraday's observations of acoustic streaming

Three steps forwards, two back, this is the way the progress of science is sometimes presented: one step after the other, regularly coming back to fundamental works to go forward in a strict and confident way. This can also be a first picture of acoustic streaming, in which a progressive motion originates from an oscillating one. But acoustic streaming is not only kinematics and has been the subject of numerous studies since the observations of Faraday (1831) reported by Rayleigh (1884): 'In these problems the fluid may be treated as incompressible. . . It was discovered by Savart that very fine powder does not collect itself at the nodal lines, as does sand in the production of Chladni's figures, but gathers itself

© The Author(s), 2025. Published by Cambridge University Press.

https://doi.org/10.1017/jfm.2025.10791 Published online by Cambridge University Press

into a cloud which, after hovering for a time, settles itself over the places of maximum vibration'. Rayleigh also identifies two ingredients of acoustic streaming, namely viscous dissipation and nonlinearity: 'This is not, perhaps, a matter for surprise, when we consider that such currents, involving as they do circulation of the fluid, could not arise in the absence of friction, however great the extent of vibration. . . we have no chance of reaching an explanation if, as is usual, we limit ourselves to the supposition of infinitely small motion and neglect the squares and higher powers of mathematical symbols by which it is expressed'.

After a few decades, technological developments in the field of sound generation led to the observation of acoustic streaming induced by sound beams propagating in the bulk of the fluid domain. Interestingly, the important paper by Eckart (1948) puts forward the intimate link between the observed flows and vorticity introduced by the acoustic excitation. Sir J. Lighthill (1978) gives an exhaustive picture in an amusing zoology of the different configurations: Stuart streaming, Rayleigh–Nyborg–Westervelt streaming and McIntyre streaming. Lighthill (1978) highlights the central part played by sound attenuation and Reynolds stresses. Still more recent technological challenges in the field of cooling (Fand & Kaye 1960; Michel & Gissinger 2021) and lighting (Dreeben & Chini 2011), but also thermoacoustics (Daru *et al.* 2021) and microfluidics (Karlsen, Augustsson & Bruus 2016), have shown this framework had to be extended to explain some experimental observations. This lead to the identification of baroclinic streaming, in which gradients in background density play the central role and acoustic attenuation is not so essential. We inherit a field of acoustic streaming fractured into three panels in the following tryptic:

(i) baroclinic streaming occurs when a standing acoustic wave is crossed with a strong density gradient (alternatively a compressibility gradient Karlsen *et al.* 2016);
(ii) Rayleigh–Schlichting streaming is observed when a standing wave interacts with a wall; note the comprehensive theoretical description by Hamilton, Ilinskii & Zabolotskaya (2003);
(iii) Eckart streaming is observed when acoustic waves progress in the form of an attenuated acoustic beam in the bulk of the fluid (Eckart 1948; Moudjed *et al.* 2014; Dubrovski, Friend & Manor 2023).

Since they describe in a single continuous parameter space both Rayleigh–Schlichting and baroclinic streaming, Mushthaq, Michel & Chini (2025) make a decisive step forward into the frontiers between the panels of this tryptic.

2. Three panels in the picture

In their paper, Mushthaq *et al.* (2025) propose a local approach featuring a multi-scale expansion of the different fields appearing in the compressible Navier–Stokes equations. They recall that the forcing yielding acoustic streaming is essentially similar to a Reynolds stress mechanism in which the fluctuating velocity of Reynolds decomposition is replaced by the rapidly oscillating acoustic velocity, and also that some acoustic vorticity is required to get a rotational forcing of the steady flow. Time averaging then enables separation of the slow dynamics of the observed flow from the comparably very fast acoustic scales. Let us adopt a two-dimensional global standpoint to consider the transverse and longitudinal scales at which the acoustic vorticity is expressed. These scales change from one panel of the tryptic to the other (see figure 1). In this global and heuristic standpoint, let us focus on the longitudinal component of the acoustic momentum $\rho_0 u'$, with u' the longitudinal

https://doi.org/10.1017/jfm.2025.10791 Published online by Cambridge University Press

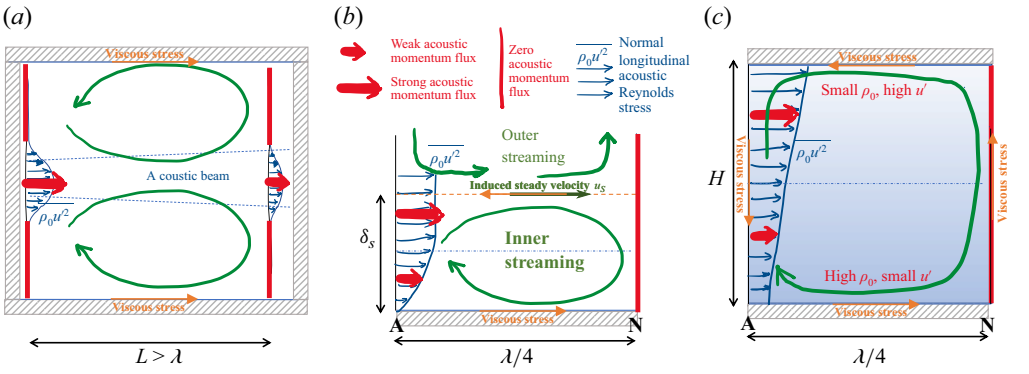


Figure 1. Acoustic streaming seen as a tryptic: each panel depicts a particular type of streaming. The represented control volume is chosen to fit the scales of longitudinal and transverse variations in the acoustic Reynolds stress $\overline{\rho_0 u'^2}$. This illustrates how a torque is induced by differences in acoustic momentum flux through the boundaries. Each type of streaming differs by the origins and scales of Reynolds stress variations. (*a*) Eckart streaming: acoustic waves propagate in the form of a beam. Transverse variations are inherent to the beam shape. Longitudinal variations are due to sound attenuation. (*b*) Rayleigh–Schlichting streaming: transverse variations are a consequence of the no-slip condition and by viscous diffusion at the boundary-layer scale, δ_S. Longitudinal variations at a $\lambda/4$ scale are due to the structure of the standing wave (A and N respectively denote antinodes and nodes for the acoustic velocity). (*c*) Baroclinic streaming occurs in a stratified environment. Longitudinal vibrations yield an acoustic standing wave; assuming that the acoustic momentum profile, $\rho_0 \boldsymbol{u}'$, is nearly uniform along the transverse direction, the acoustic velocity must vary inversely to the density. These variations thus occur at the scale of the cavity, H. Longitudinal variations at a $\lambda/4$ scale are due to the structure of the standing wave (A and N respectively denote antinodes and nodes for the acoustic velocity).

acoustic velocity component and ρ_0 the background density. The counterpart of the normal Reynolds stress is then the time-average momentum flux through a transverse cross-section over one acoustic period, $\overline{\rho_0 u'^2} h$, where h is the height of the cross-section considered .

In the first panel (figure 1*a*) Eckart streaming is induced by an acoustic beam in a cavity. The longitudinal scale is the length of the beam, which is given by the sound intensity attenuation length and can be far greater than an acoustic wavelength (Lighthill 1978; Moudjed *et al.* 2014; Vincent *et al.* 2024). The transverse scale is that of the cavity. The acoustic wave momentum decreases along the longitudinal direction due to attenuation, generating a forcing in the direction of propagation. The beam-shape structure yields two macroscopic torques which induce two circulating flows at the scale of the upper and lower half-cavities, respectively. A permanent regime is reached when the torques due to external viscosity forces balance these forcing torques.

In the second panel (figure 1*b*) representing the inner streaming due to a standing wave, the transverse scale is that of the acoustic boundary layer, $\delta_s = \sqrt{\mu\lambda/\rho_0\, c}$, where μ and c respectively denote the dynamic viscosity and the celerity of sound. The longitudinal scale is a quarter of a wavelength λ. The longitudinal momentum, $\rho_0 \boldsymbol{u}'$, is maximum at the antinode A of the standing velocity wave and zero at the node N. It also varies in the transverse direction due to viscous diffusion and the no-slip condition at the wall; the momentum flux into the control volume is then stronger in the upper part of the boundary layer than in the lower part. The resulting torque is expected to scale as $\overline{\rho_0 u'^2}\delta_S^2$. Denoting by u_S the order of magnitude of the steady velocity induced at the top of the boundary layer, the external viscous torque at the scale of the inner recirculation is of the order of $(\mu u_s/\delta_S)\lambda\delta_S$. Balancing one torque by the other yields $u_S \sim \overline{u'^2}/c$, which also gives the

https://doi.org/10.1017/jfm.2025.10791 Published online by Cambridge University Press

scaling of the flow induced in the bulk referred to as Rayleigh streaming. Remarkably, u_S does not depend on the aspect ratio δ_S/λ.

The third panel (figure 1*c*) is the one of most interest today. Imagine that, prior to the Rayleigh–Schlichting experiment depicted in figure 1(*b*), heating from above leads to a strong stratification in background density ρ_0 (Lin & Farouk 2008; Michel & Gissinger 2021). Introducing longitudinal oscillations would induce a standing wave. In a one-way coupling approximation, the background density is not affected by the wave. Assuming that the fluctuating pressure is approximately uniform across the channel, the longitudinal acoustic momentum, $\rho_0 \boldsymbol{u}'$, is also nearly uniform. The amplitude u' of the acoustic velocity must then vary inversely to ρ_0. This induces, at the antinode A, a strong transverse gradient in the time-averaged momentum flux into the control volume. The consequent powerful torque at the scale of the cavity, H, creates a single global recirculation directed towards the antinode A on the side of the heavier fluid. This is a very different picture than the outer recirculations of Rayleigh streaming, flowing towards the nodes near the walls, and which are driven by a smaller recirculation induced at the boundary-layer scale where the acoustic torque applies. Here, the balance by the steady external viscous torque involves the four sides of the control volume and is thus directly dependent on its aspect ratio $\delta = 4H/\lambda$.

These back-of-the-envelope explanations certainly miss several significant effects, for instance the momentum flux associated with the transverse component of the acoustic velocity, v', at the top of the boundary layer and the modification of the background density by the flow (the coupling actually appears to be a two-way coupling). Our contention, however, is that they give a qualitatively correct picture of the mechanisms at play. The distinction between the mechanisms in figures 1(*b*) and 1(*c*) is indeed very thin since baroclinic streaming occurs as soon as the gradient in fluid properties is such that a torque occurs. That is to say that transverse and longitudinal variations in acoustic momentum are combined. As this baroclinic, time-averaged, torque acts at the cavity scale while Rayleigh–Schlichting is created in thin boundary layers, it is very efficient even in a weak stratification. Starting from a state of pure Rayleigh streaming, progressively increasing the heating, i.e. the stratification, until baroclinic streaming becomes significant chases the boundary between figures 1(*b*) and 1(*c*) away. This is what Mushthaq *et al.* (2025) do using a local approach for a small level of heating.

3. Baroclinic transition in acoustic streaming: beyond Rayleigh's paradigm

More specifically, Mushthaq *et al.* (2025) consider standing acoustic wave oscillations of an ideal gas in a differentially heated channel with wall temperatures set to $T_* + \Delta\Theta_*$ and T_*. They consider Rayleigh streaming and baroclinic streaming as two asymptotic regimes for $\Delta\Theta_* \sim 0$ and $\Delta\Theta_* = O(T_*)$, respectively. Their small parameter is a normalised temperature difference, $\Gamma = \Delta\Theta_*/T_*$, assumed comparable to the acoustic Mach number. As illustrated in their figure 2, their equation (3.56) for the streamfunction describes the steady flow between the node and antinode cross-sections as the superimposition of 3 components:

(i) two Rayleigh streaming cells corresponding to the isothermal flow and exhibiting the expected symmetry with respect to the middle plane;
(ii) one baroclinic streaming recirculation driven by the heating-induced density gradient, expectedly spanning the entire height of the channel;
(iii) a small corrective term depending on the type of forcing, an oscillating body force or an oscillating wall.

https://doi.org/10.1017/jfm.2025.10791 Published online by Cambridge University Press

As this analytical solution elucidates the separate contributions of viscous torques in the boundary layers and baroclinic forcing in the bulk, the authors can investigate the typical value Γ_c over which baroclinic streaming becomes dominant, as shown in their equation (4.8). Remarkably, Γ_c does not depend on the forcing amplitude and is composed of three factors; the acoustic Reynolds number (the ratio of the wavelength times the sound celerity to the fluid kinematic viscosity), a term featuring the ideal gas properties only and a function of the aspect ratio δ only. This typical value Γ_c behaves as δ^{-2} for narrow chanels and as $\delta^{1/2}$ for tall channels.

Of course, a lot remains to be investigated. For instance, steady horizontal density gradients induced in this two-way coupling are a motor for buoyancy-driven convection whose magnitude relative to baroclinic streaming should be assessed. This type of forcing could also be situated with respect to thermo-vibrational convection. Eckart acoustic streaming could be coupled with strong background gradients in mechanical properties, etc. Mushthaq *et al.* (2025) significantly improve the understanding of flows driven by sound waves. Experimentalists will be enlightened in designing their set-ups and theoreticians will be inspired by this smart approach. Modern applications of acoustofluidics, think of biomedical applications for instance (Baudoin & Thomas 2020), often combine several types of streaming flows and similarly will benefit from the new insights provided by Mushthaq *et al.* (2025). These insights are not restricted to acoustic streaming, of course, nor to engineering applications: for instance, communities working on other types of steady streaming or on geophysical configurations, think of internal waves (Dauxois *et al.* 2018), could well be inspired too. Chasing the boundary between Rayleigh and baroclinic streamings away, Mushthaq *et al.* (2025) definitely take an important step forward.

Acknowledgements. Warm thanks to S. Miralles for her help in writing this paper. Many thanks to G. Michel for the friendly and fruitful discussions, to G. Chini and J. Neufel for the thorough review of the initial draft and also to J. Magnaudet for the encouraging discussion at EFDC2.

References

Baudoin, M. & Thomas, J.L. 2020 Acoustic tweezers for particle and fluid micromanipulation. *Ann. Rev. Fluid Mech.* **52** (1), 205–234.

Daru, V., Weisman, C., Baltean-Carlès, D. & Bailliet, H. 2021 Acoustically induced thermal effects on Rayleigh streaming. *J. Fluid Mech.* **911**, A7.

Dauxois, T., Joubaud, S., Odier, P. & Venaille, A. 2018 Instabilities of internal gravity wave beams. *Ann. Rev. Fluid Mech.* **50** (1), 131–156.

Dreeben, T.D. & Chini, G.P. 2011 Two-dimensional streaming flows in high-intensity discharge lamps. *Phys. Fluids* **23** (5), 056101.

Dubrovski, O., Friend, J. & Manor, O. 2023 Theory of acoustic streaming for arbitrary Reynolds number flow. *J. Fluid Mech.* **975**, A4.

Eckart, C. 1948 Vortices and streams caused by sound waves. *Phys. Rev.* **73**(1), 68–76.

Fand, R.M. & Kaye, J. 1960 Acoustic streaming near a heated cylinder. *J. Acoust. Soc. Am.* **32** (5), 579–584.

Faraday, M. 1831 On a peculiar class of acoustical figures; and on certain forms assumed by groups of particles upon vibrating elastic surfaces. *Phil. Trans. R. Soc. Lond.* **121**, 299–340.

Hamilton, M.F., Ilinskii, Y.A. & Zabolotskaya, E.A. 2003 Acoustic streaming generated by standing waves in two-dimensional channels of arbitrary width. *J. Acoust. Soc. Am.* **113** (1), 153–160.

Karlsen, J.T., Augustsson, P. & Bruus, H. 2016 Acoustic force density acting on inhomogeneous fluids in acoustic fields. *Phys. Rev. Lett.* **117** (11), 114504.

Lighthill, S.J. 1978 Acoustic streaming. *J. Sound Vib.* **61** (3), 391–418.

Lin, Y. & Farouk, B. 2008 Heat transfer in a rectangular chamber with differentially heated horizontal walls: effects of a vibrating sidewall. *Intl J. Heat Mass Transfer* **51** (11), 3179–3189.

Michel, G. & Gissinger, C. 2021 Cooling by baroclinic acoustic streaming. *Phys. Rev. Appl.* **16** (5), L051003.

https://doi.org/10.1017/jfm.2025.10791 Published online by Cambridge University Press

MOUDJED, B., BOTTON, V., HENRY, D., BEN HADID, H. & GARANDET, J.P. 2014 Scaling and dimensional analysis of acoustic streaming jets. *Phys. Fluids* **26** (9), 093602.

MUSHTHAQ, R., MICHEL, G. & CHINI, G.P. 2025 Baroclinic transition in acoustic streaming: beyond Rayleigh's paradigm. *J. Fluid Mech.* **1017**, A32.

RAYLEIGH, L. 1884 On the circulation of air observed in Kundt's tubes, and on some allied acoustical problems. *Phil. Trans. R. Soc. Lond.* **175**, 1–21.

VINCENT, B., HENRY, D., KUMAR, A., BOTTON, V., POTHÉRAT, A. & MIRALLES, S. 2024 Phenomenology of laminar acoustic streaming jets. *Phys. Rev. Fluids* https://hal.science/hal-04674347 submitted for publication.

https://doi.org/10.1017/jfm.2025.10791 Published online by Cambridge University Press